*Desalination and Water Treatment*
www.deswater.com

doi: 10.5004/dwt.2020.26309

205 (2020) 328–335
November

# Application of erionite as an adsorbent for $Cd^{2+}$, $Cu^{2+}$, and $Pb^{2+}$ ions in water

Waheed Ahmad Khanday[a], Suhail Ahmad Khanday[b], Mohammed Danish[c,*]

[a]*Department of Chemistry, Government Degree College, Anantnag 192102, Jammu and Kashmir, India, email: khanday.waheed@yahoo.com (W.A. Khanday)*
[b]*Department of Civil Engineering, National Institute of Technology, Silchar, Assam, India, email: khandaysuhail2013@gmail.com (S.A. Khanday)*
[c]*Bioengineering Technology Section, Universiti Kuala Lumpur Malaysian Institute of Chemical and Bioengineering Technology, Universiti Kuala Lumpur, Alor Gajah 78000, Melaka, Malaysia, email: mdanish@unikl.edu.my (M. Danish)*

Received 4 July 2019; Accepted 30 June 2020

**ABSTRACT**

Erionite was synthesized by the hydrothermal method using NaOH, KOH, tetramethylammonium chloride, and silica sol. The synthesized erionite was characterized for materials crystal/amorphous properties, surface morphology, functional groups, and surface area measurements. The synthesized and characterized composite material was used for the scavenging of the $Cd^{2+}$, $Cu^{2+}$, and $Pb^{2+}$ ions in the aqueous medium. The scavenging behavior of erionite towards $Cd^{2+}$, $Cu^{2+}$, and $Pb^{2+}$ ions was evaluated in a batch adsorption process. The process variables, such as initial metal ions concentration ($10^{-8}$ to $10^{-5}$ mol/L), solution pH (2–10), and temperature (30°C–50°C) were varied within the selected range to observe the effect of each variable. The best fitting of the adsorption isotherm data in the isotherm (Langmuir and Freundlich isotherm) models were decided according to correlation coefficient ($R^2$), root mean square error (RMSE), and standard deviation (SD) values. According to Langmuir, the highest uptakes for $Cd^{2+}$, $Cu^{2+}$, and $Pb^{2+}$ metal ions at 50°C were 258.71, 265.41, and 275.73 mg/g, respectively. The maximum sorption of $Cd^{2+}$, $Cu^{2+}$, and $Pb^{2+}$ on synthesized erionite was achieved in the pH range 6.0–8.0. Sorption of metal ions was found to be enhanced with the rise of adsorbent dosage. Sorption isotherm data were followed Freundlich model according to $R^2$, RMSE, and SD values.

*Keywords:* Erionite; Hydrothermal method; Sorption; Isotherms; Trace metal ions

## 1. Introduction

The natural composition of inland and underground aquifers water is contaminated above the bearable limits with the trace metals through anthropological activities and waste disposal of industrial discharge. The trace metal-contaminated water causes a serious threat to the environment owing to its high toxicity. The consumption of $Cd^{2+}$ ions through water or food causes the respiratory disorder, hypertension, and kidney and liver failure in humans [1]. The cadmium toxicity is also associated with itai–itai disease in humans [2], the phytotoxicity effect of $Cd^{2+}$ ions has been recognized by the researchers and reported in the literature [3]. The leakage of $Pb^{2+}$ ion in potable water can damage many organs and tissues in human beings such as bones, kidneys, intestines, hearts, reproductive, and central nervous [4]. The $Cu^{2+}$ ingestion in the human body through direct or indirect means can cause regurgitate, hematemesis (spewing up blood), low blood pressure, jaundice, gastrointestinal distress, and even death [5,6]. Hence, scavenging of Cd, Cu, and Pb from water and wastewater is essential for ensuring better health in human beings.

The conventional practice for metals and heavy metal ions scavenging from an aqueous medium includes

* Corresponding author.

oxidation, reduction, precipitation, ion exchange, and adsorption methods. The trend changed in the recent decade by using adsorption as a most powerful tool for scavenging of heavy metal ions from contaminated water. The use of various abundantly available and economically viable adsorbents sorbents such as hazelnut shell [7], cassava waste [8], peat [9], and date stone activated carbon [10] have been reported for the remediation of Cd, Cu, Zn, and other heavy metal ions in contaminated water. In the recent past, many researchers reported agricultural wastes with certain modifications in it as an effective adsorbent against metal ions. The rice husk was burnt, and its ash was used for the scavenging of the Cd(II) and Zn(II) from its binary solution of wastewater [11]. The rice straw modified with compost was used against the Cd(II) and Cu(II) in soil [12] and rice straw without any modification was used as biosorbent for the remediation of Cd(II), Zn(II), Cd(II) and Hg(II) from industrial wastewater [13]. Sawdust and neem bark was also used as an adsorbent for zinc(II) and cadmium(II) removal [14]. Dairy manure was converted to biochar for scavenging of the Cu, Zn, and Cd ions [15]. Polymer nanocomposite was synthesized by Badruddoza et al. [16] for the selective separation of heavy metals from wastewater. Nontronite hybrid surface was found effective against an aqueous solution of divalent toxic metals ions [17]. Nano-crystalline calcium hydroxyapatite was synthesized and applied against the Ni(II) ion [18]; the adsorption capacity was reported to be 46.17 mg/g. In contemporary research, the zeolite and zeolite composites are used as an adsorbent against metal ions. The natural zeolite was used against heavy metals present in acid mine drainage [19]. Shyaa et al. [20] prepared a nano-composite from natural zeolite and polyaniline for Cr(VI) ions removal from wastewater. The adsorption efficiency of zeolite-like materials was encouraged for synthesizing such adsorbents. In our previous studies, we have used mica mineral clintonite [21] for the removal of heavy metal ions and modified zeolite laumontite [22] for removal of oxo-anions from wastewater.

Erionite is a synthetic zeolite like materials, having surface area 350 $m^2/g$, and suitable surface characteristics for adsorption. These characteristics of high porosity and surface area make it the best client for adsorption of metal ions like $Cd^{2+}$, $Cu^{2+}$, and $Pb^{2+}$ ions. Also upon the comparison of erionite with the previously used adsorbents in the literature [23–30], its removal capacity has been found to be quite high and this validates the idea of using it as a new adsorbent. It further paves a way for other researchers to prepare new mica minerals to be used as adsorbents. The experiment of this study will be focused on the effect of contact time, the effect of pH, effect erionite dosage, and initial concentrations of metal ions. The isotherm parameters were also calculated, for predicting the adsorption behavior of the erionite against the selected metal ions.

## 2. Experimental

### 2.1 Reagents and chemicals

The following chemicals were procured from Sigma-Aldrich (India) of analytical grade. (1) Anhydrous sodium aluminate (50%–56% $Al_2O_3$, 0.05% $Fe_2O_3$, 40%–45% $Na_2O$), (2) silica sol, (3) sodium hydroxide 99.998%, (4) tetramethylammonium chloride (TMA) Cl 99%, (5) potassium hydroxide 99.998%, (6) sodium acetate 99.6%, (7) potassium chloride 99.8%, (8) cadmium nitrate, (9) lead nitrate, and (10) copper nitrate. The de-mineralized (DM) water used during the experiment was taken from Milli Q lab grade water purifier. All these reagents were used for the purest quality.

### 2.2. Procedure for erionite synthesis

Erionite adsorbent was prepared in batch, for each batch 6 g NaOH and 15 g KOH was mixed in 25 mL of demineralized water. The 10 g of sodium aluminate was added to the mixture of a solution of NaOH and KOH, then set for heating and continuous stirring at a boiling point till a clear solution was obtained. The clear solution was put in a desiccator to cool down at room temperature, the cooling solution was stirred vigorously, and a saturated solution of 11 g of tetramethylammonium chloride (a site directing agent) was added drop by drop while stirring the solution. The silica sol solution was prepared in a separate beaker by stirring 90 g silica sol and 115 mL demineralized water for an hour. The silica solution was mixed with the previously prepared complex mixture, after mixing it forms a thick gel. The gel was kept in a polypropylene bottle for 2 h at room temperature; then bottles were transferred to Teflon lined autoclave that kept on preheating at 172°C for 72 h. After autoclaving the materials, it transferred to cold water for washing and centrifuged till pH ≤ 9 was achieved [31]. The washed material dried at 110°C in a hot air oven overnight. The obtained material was in agglomerated form. Therefore, grounded into powder form then calcined at temperature 540°C for 7 h to remove volatile organic matters from it, and form a stable material.

### 2.3. Instrumental analysis of synthesized of erionite

The crystallinity and amorphocity of the erionite material were tested through powder X-ray diffraction (XRD) study. The erionite representative samples were sieved in an ABNT n° 200 (0.074 mm) sieve before place in diffractometer (Shimadzu XRD 6000, Japan). The powder X-ray diffraction study was run with Cu K$\alpha$ radiations at 40 KV/30 mA. The scanning of 2$\theta$ was selected in the range of 2°–70° with a step of 0.02°. The only *d*-spacings of concern in the X-ray diffractogram was the basal spacings along the *c*-axis.

The functional groups in the erionite samples were determined through the Fourier transformed infrared (FTIR) analysis. The sample was grounded with KBr in the weight ratio of 1:5 and was compressed into a translucent thin film. The spectrum of the sample was collected through the Shimadzu FTIR (Japan) in the wavelength range of 4,000–400 $cm^{-1}$, with a scan rate of 4 $cm^{-1}$.

The surface textural properties of the erionite were analyzed through the nitrogen adsorption–desorption method (using Autosorb 2120 instrument). The surface area was calculated through Brunauer–Emmet–Teller (BET) method, and pore size distribution was also measured.

Surface micrograph of erionite was obtained by JEOL JSM 5800 (USA), scanning electron microscopy with energy dispersive X-ray analysis (SEM-EDAX) instrument. Scanning electron micrograph of erionite was taken at 10,000×

magnification for the vivid representation of surface morphology. The energy dispersive X-ray spectroscopy (EDS) was carried out to identify the elemental composition of the erionite surface. The erionite sample for EDS analysis was prepared through a surface coating method to avoid charge influence.

### 2.4. Sorption studies

#### 2.4.1. Solution preparation

Low concentration solutions (200 mg/L) of $Cd^{2+}$, $Cu^{2+}$, and $Pb^{2+}$ were prepared in deionized water from their respective nitrates and filtered through a whatmann micro-filter (0.45 μm). Filtrates were acidified by adding 1 mL $HNO_3$/L solution. The filtrate acidity should be maintained between the pH 1.7 and 2.0. The sample solution usually digested before voltammetric determination of concentrations, because the presence of organic matter often interferes during analysis.

#### 2.4.2. Sorption experiment

The sorption of trace metal ions by erionite was conducted through a batch experiment mode. Batch sorption was conducted by taking 100 mg of sorbent in 250 mL conical flask having 25 mL of solutions containing metal ions ($Cd^{2+}$, $Cu^{2+}$, and $Pb^{2+}$) of 200 mg/L concentrations at constant temperatures (30°C). To observe the effect of pH on the sorption the pH of the solution was controlled with the help of 0.1 N HCl and 0.1 N NaOH solutions. The conical flasks were shaken in a thermostat water bath with orbital shaking system at agitation speed of 125 rpm. After a stipulated time of shaking the sorbate and sorbent solutions were separated. The concentration of $Cd^{2+}$, $Cu^{2+}$, and $Pb^{2+}$ ions in residual water samples before and after adsorption were determined by means of anodic stripping voltammetry (ASV) using 797 VA computrace ion analyzer.

The equilibrium adsorption amount, $q_e$ (mg/g), was determined by:

$$q_e = \frac{\left(C_i - C_f\right)V}{W} \tag{1}$$

where $C_f$ (mg/L) and $C_i$ (mg/L) represents the final and initial concentration of metal ions, respectively. The erionite adsorbent mass is denoted by W (g) and volume of solution by $V$ (L).

## 3. Result and discussion

### 3.1. Characterization of erionite

The crystallinity of the synthesized erionite was analyzed through the powder X-ray diffractometer. The X-ray diffraction pattern of calcined erionite is published somewhere else [32], the diffractogram pattern affirm that erionite is crystalline. The significant sharp peaks in the diffractogram patterns of erionite appear at 2θ of 7°, 13.5°, 19°, 24°, and 29.5° which closely resemble with all catalytic forms of erionite, that already reported in the literature of erionite zeolite [32].

The surface functional groups of the erionite adsorbent were identified through the FTIR spectroscopy using KBr pallets method. The broad transmission peak at 3,470 $cm^{-1}$ was due to the O–H bonding, and the transmission peak at wavenumber 450 $cm^{-1}$ was due to Si, Al–O bond [32]. The transmission peak at 1,000 and 750 $cm^{-1}$, were due to asymmetric and symmetric stretches of bonds in the zeolite molecules, respectively. The transmission peak at 1,480 $cm^{-1}$ may be due to M–OH, where M is balancing metal in the zeolite framework. The (C=N) deformation of an organic template (TMA) used during erionite synthesis was observed at wavenumber 1,700 $cm^{-1}$.

The nitrogen adsorption–desorption curve was used to calculate the surface area of erionite, the BET surface area was found to be around 350 $m^2/g$ [32], which is very closure to the characteristics of the zeolites. The BJH analysis was used to calculate the pore size distribution in the erionite; the pore diameter was found to be varied in the range of 6–10 nm. These pores belong to the mesopore range according to International Union of Pure and Applied Chemistry (IUPAC) definition; the porous materials can be categorized into three types: micropore (diameter < 2 nm), mesopore (2–50 nm), and macropore (>50 nm), the erionite prepared in this study contains a higher percentage of mesopores.

The surface morphology of erionite was captured through the FESEM images. It can be seen from the image the erionite surface appears to have relatively non-uniform distribution of molecules, lightly uneven pore morphology with varying particle size [32]. It appears under the scanning electron microscopy as chunks and sometimes as spheres of 5–10 μm.

The surface elemental composition of the erionite was observed through the EDS peaks. The results showed peaks for elements like Al, Ca, K, Na, O, and Si. The percentage of elements showed that O is present with the highest percentage, which is almost half of the total elements present at the surface by weight. The percentage of the Si was found higher than the Al atoms; this confirms the Si/Al ratio was greater than 1, which was taken during the synthesis of erionite. Moreover, the atomic ratio of the Si/Al is in accordance with the molar ratio of the Si and Al solutions taken during the synthesis.

### 3.2. Metal sorption studies

The post adsorption residual concentrations of $Cd^{2+}$, $Cu^{2+}$, and $Pb^{2+}$ ions in the filtrate were determined using ASV using 797 VA computrace ion analyzer. All the voltammograms were recorded using the parameters given in Table 1.

#### 3.2.1. Effect of time

For the kinetic study of metal ions mass transfer from solution to the solid surface of erionite, time was varied between 4 and 24 h keeping rest of the parameters constant (pH 7, temperature 30°C, and adsorbent dosage 100 mg). The kinetic plots were shown in Fig. 1, represents the trace metals (Cd, Cu, and Pb) ion sorption on synthesized erionite adsorbent. The kinetics plots are shown vividly that the sorption of selected metal ions has increased up to 8 h

Table 1
Parameters of voltammograms

| Parameters | Variables chosen |
|---|---|
| Working electrode | HMDE |
| Stirrer/RDE | 2,000 rpm |
| Drop size | 4 |
| Measurement mode | DP |
| Purging time | 200 s |
| Pulse amplitude | 0.05 V |
| Deposition potential | –0.05 V |
| Deposition time | 90 s |
| Equilibration time | 20 s |
| Start potential | –0.09 V |
| End potential | –0.1 V |
| Voltage step | 0.006 V |
| Sweep rate | 0.015 V/s |

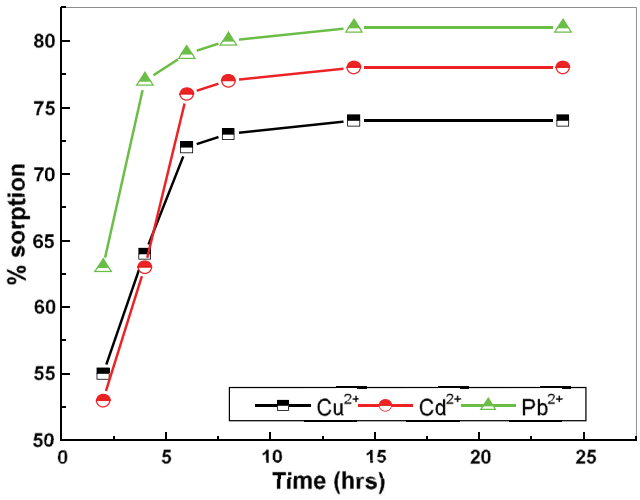


Fig. 1. Kinetics for sorption of metal ions onto erionite (pH 7, temperature 30°C, agitation speed = 125 rpm, and sorbent concentration 100 mg).

of contact time after that saturation appears and adsorption–desorption rate became equal. Hence, 8 h of contact time was taken as equilibrium time in this study. The slow and steady increase in sorption with contact time can be attributed to the slow interaction of the erionite solid surface and solvated metal ions concentrations. The concentration difference between metal ions in the bulk solution and solid–liquid interface of the erionite was served as a driving force to carry the solvated metal ions from solution to erionite solid surface. It was observed that in the first 6 h, the sorption rate was higher for all the three metal ions, then slow down and reached equilibrium. The initial higher rate of metal ions sorption attributed to the vacant sorption sites as well as the concentration differences of the metal ions at the erionite surface and in the bulk of solution was large. Whereas, after 6 h of contact time, the sorption rate decreased significantly due to slowing down of the diffusion rate of cations into the interior channels of erionite. The diffusion rate was guided by the surface coverage of the metal ions, once the erionite surface was saturated with the metal ions, the diffusion rate decreased. It can be seen from Fig. 1, after 8 h of contact time, there was a negligible or slight change in the sorption of metal ions. Therefore, 8 h was established as equilibrium time for $Cd^{2+}$, $Cu^{2+}$, and $Pb^{2+}$ ions adsorption onto erionite, for further experiments in this study this equilibrium time was used.

### 3.2.2. *Effect of pH*

The $pH_{pzc}$ is the pH where the adsorbent net surface charge corresponds to zero, and it offers the possible mechanism about the electrostatic interaction between adsorbent and adsorbate. For the point of zero charge ($pH_{pzc}$) determination the initial pH ($pH_i$) of aqueous solutions (100 mL) were adjusted to a pH range of 2–12 using 0.1/1.0 M HCl or NaOH. Then, 0.1 g of erionite was added to each adjusted solution. The dispersions were shaken for 48 h at 30°C, and the final pH of the solutions ($pH_f$) was determined. The point of zero charge ($pH_{pzc}$) is the point where the curve $pH_f$ vs. $pH_i$ intersects the line $pH_f = pH_i$ and from this the $pH_{pzc}$ value of 6.1 was obtained for erionite. The sorption of metal ions as a function of pH was studied at temperature 30°C and adsorbent dosage 150 mg/L. In the selected range of pH (from 2–10) for this study, it was observed that for $Cd^{2+}$ and $Cu^{2+}$ adsorption on to the erionite was increased till pH 8.0 then decreased. Whereas, for $Pb^{2+}$ ions, the maximum adsorption achieved at pH 6.0 (as shown in Fig. 2). Because of $pH_{pzc}$ value of 6.1 for erionite, the maximum sorption of $Cd^{2+}$, $Cu^{2+}$, and $Pb^{2+}$ ions on synthesized erionite is found at pH 6.0–8.0 as a consequence of the increase in electrostatic interactions between the metal cations and erionite due to deprotonation of surface active sites. The decrease in adsorption at higher pH may be explained due to the formation of bulky hydroxide complexes at higher pH. At low pH (pH 2), the sorption was very low because it is known that acids affect the structure of mica minerals. In mica mineral frameworks, the Si–O–Al bonds are weaker than Si–O–Si bonds, hence it can easily be attacked by $H^+$ ions affecting their structure. The extent of damage in the structure of mica minerals depends on the strength of the acids. The geometrical arrangement of the atoms in zeolites and clays, particularly with small Si/Al ratios, may collapse in the presence of acids with pH lower than 5. The intensity of the pH effect is more pronounced on the structure of the zeolites and clays at pH < 3.0. The decrease in the sorption percent in high acidic solution (low pH) can be attributed to the collapse of the structural network of the adsorbents. The surface of the erionite would be closely associated with hydronium ions ($H_3O^+$) in high acidic solutions (low pH) that hindered the access of metal ions to the adsorbent (erionite) surface; this may be another possible reason for the decrease in the sorption capacity of erionite in high acidic solution. Similar charges in adsorbate (metals ions) and adsorbent surface (due to the presence of $H_3O^+$ ions) was causing electrostatic repulsion. Consequently, the sorption was found to be decreased. With the rise of pH of the solution, negative charged ($OH^-$) ions increased, and positively charged ions decreased at the surface of erionite, which results in an attractive force between

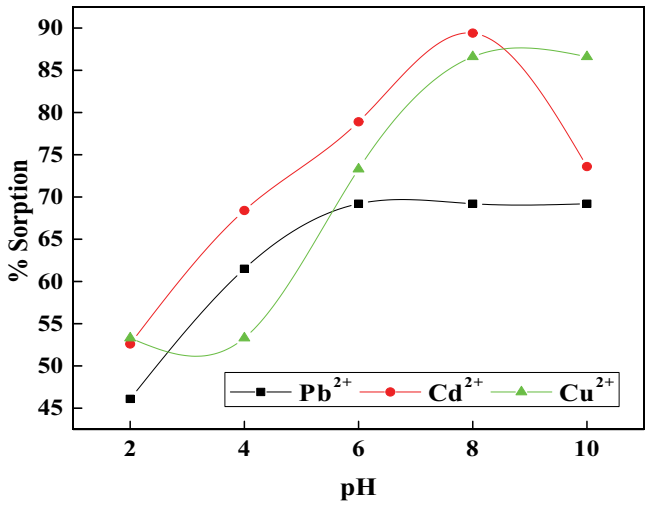


Fig. 2. Effect of pH on the sorption of metal ions onto erionite (temperature 30°C, agitation speed = 125 rpm, and sorbent concentration 100 mg).

the metal ions and the surface of the erionite. Hence, the adsorption capacity of the erionite was found to be increased at higher pH.

### 3.2.3. Effect of erionite dosage and initial metal ions concentrations

The change in the erionite dosage (g/L) for fixed initial concentrations of the metal ions was helped in observing the effect of adsorbent dosage. The sorption of metal ions was observed to be enhanced with an increase in sorbent dosage; it was due to an increase of sorption sites with the rise of sorbent dosage. In other sets of experiments, the metal ion concentration was varied, and its effect was observed on a fixed dosage of the sorbent. The experimental results showed that the sorption percentage of metal ions decreased with an increase in metal ion concentration ($10^{-8}$ to $10^{-5}$ mol/L). It can be explained in terms of available sorption sites are limited in the solution for higher metal ions concentrations.

### 3.2.4. Adsorption isotherms

The sorption isotherm will help in understanding the sorbent–sorbate relationship, and molecular distributions of the sorbate molecules at the surface of the sorbent at equilibrium. The isotherm will also predict the maximum sorption capacity of the sorbent under given conditions. The maximum sorption capacity of the sorbent can be predicted by applying the isotherm data to various established isotherm models such as Langmuir (for monolayer sorption) and Freundlich (for multilayer sorption) models. In this study, Langmuir and Freundlich isotherms were modeled to simulate the obtained data of metal ion ($Cd^{2+}$, $Cu^{2+}$, and $Pb^{2+}$) sorption onto erionite. Langmuir model [33] assumes the sorbent surface as homogeneous having identical surface sites with almost equal energy. Its nonlinear form can be expressed as:

$$q_e = \frac{q_m K_L C_e}{1 + K_L C_e} \tag{2}$$

the linearized form of Langmuir isotherm can be expressed as:

$$\frac{C_e}{q_e} = \frac{C_e}{q_m} + \frac{1}{K_L q_m} \tag{3}$$

where $K_L$ (L/mg) is constant of sorption associated with free energy, $q_m$ (mg/g) denotes the maximum sorption capacities, and $C_e$ (mg/L) represents the equilibrium concentrations of metal ions. Applicability of Freundlich isotherm [34] describes the multilayer sorption process. This isotherm was developed by presuming the heterogeneous sorbent surface with nonuniform surface energy distribution. The nonlinear form of Freundlich isotherm can be expressed as:

$$q_e = K_F C_e^{\frac{1}{n}} \tag{4}$$

The linearized form of Freundlich isotherm can be expressed as:

$$\ln q_e = \ln K_F + \frac{1}{n} \ln C_e \tag{5}$$

where $n$ and $K_F$ (mg/g) $(L/mg)^{1/n}$ are Freundlich parameters for the sorption intensity and sorption capacity, respectively. The isotherm data at 30°C, 40°C, and 50°C was applied to the non-linear form of isotherm models represented in Eqs. (2) and (4) for the sorption of metal ions onto erionite (Fig. 3). Root mean square errors (RMSE) in the isotherm model was calculated to evaluate the error in the model parameters. The following equation was used for the RMSE calculation:

$$\text{RMSE} = \sqrt{\frac{\sum_1^p (q - q_m)^2}{p}} \tag{6}$$

where $q$ is experimental sorption capacity, $q_m$ is model predictions sorption capacity, and $p$ denotes the number of data points.

Standard deviation (SD) in the data were calculated to determine the validity of models by the following expression:

$$S.D. = \sqrt{\frac{\Sigma[(q - q_m)/q}{n - 1}} \tag{7}$$

where $q_m$ and $q$ represent the calculated and experimental sorption capacities, and $n$ is the total number of data points. The Freundlich and Langmuir parameters such as $K_F$, $1/n$, $K_L$, and $q_m$, were determined by the linear plots using intercepts and slopes of the best fit straight line. The RMSE, SD, and correlation coefficients ($R^2$) were determined for selected metal ions (Cd, Cu, and Pb) adsorption onto erionite, to validate the isotherm models (as shown in Table 2). The lower values of RMSE (<0.05) and SD (<0.05) and higher values of $R^2$ (>0.97) will favor the applicability of the isotherm

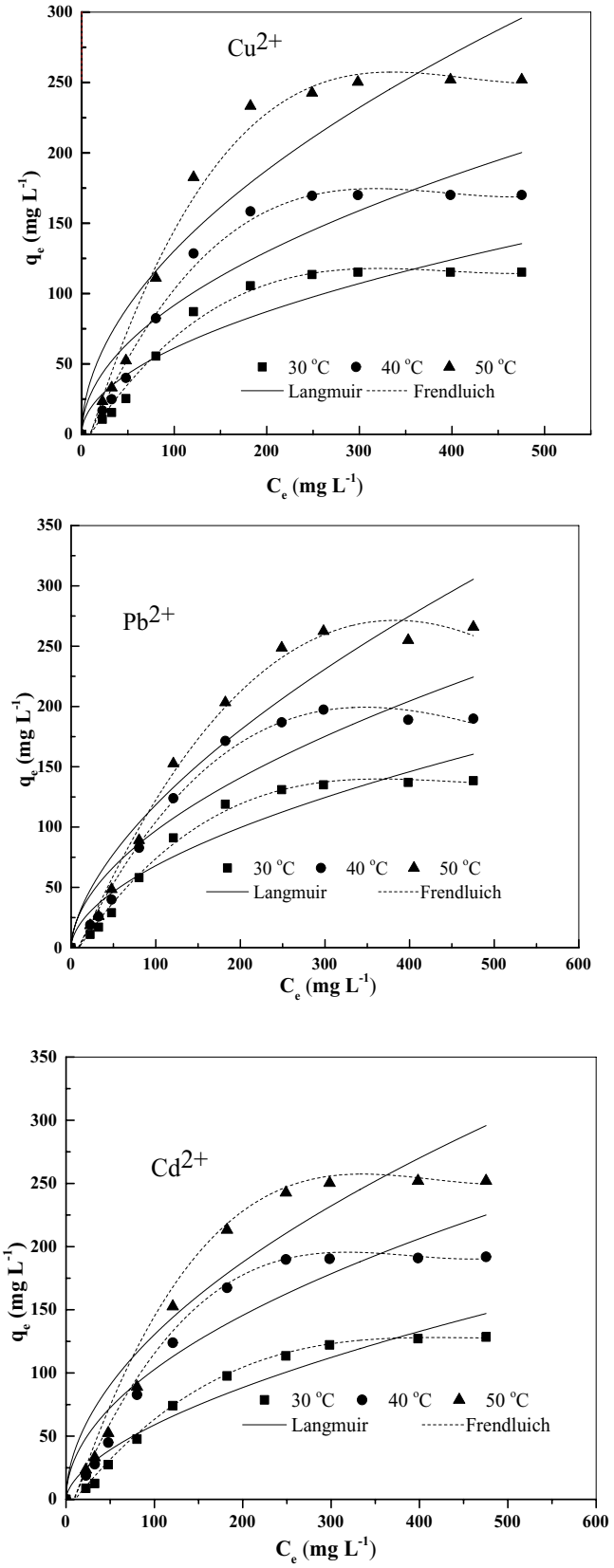


Fig. 3. Langmuir and Freundlich adsorption isotherms for adsorption of $Cd^{2+}$, $Cu^{2+}$, and $Pb^{2+}$ on erionite at different temperatures.

model. From Table 2, it can be seen that Freundlich isotherm favored by these statistical tests.

With the rise of solution temperature $q_{max}$ rises from 134.47 to 258.71 mg/g for $Cd^{2+}$, 123.17 to 265.41 mg/g for $Cu^{2+}$, and 141.41 to 275.73 mg/g for $Pb^{2+}$. Therefore, it can be inferred from the results that sorption of $Cd^{2+}$, $Cu^{2+}$, and $Pb^{2+}$ ions onto erionite was multilayered and support physisorption mechanism (as it followed Freundlich isotherm) [35]. Shen et al. [36] reported $Cd^{2+}$, $Cu^{2+}$, and $Pb^{2+}$ removal through $Fe_2O_3$@ microalgae composite, the order of the adsorption capacity following order: $Pb^{2+}$ (62.63 mg/g) > $Cd^{2+}$ (42.12 mg/g) > $Cu^{2+}$ (38.68 mg/g). Chen et al. [37] also investigated divalent metal ions removal through $MnFe_2O_4$@CAC hybrid adsorbent, the order of removal was observed in the following order: $Cu^{2+}$ (608.46 mg/g) > $Pb^{2+}$ (471.45 mg/g) > $Cd^{2+}$ (354.43 mg/g). The adsorption capacity of erionite for $Cd^{2+}$, $Cu^{2+}$, and $Pb^{2+}$ ions was found quite high on comparing with other adsorbents from literature as shown in Table 3.

The adsorption of all the three metal ions $Cd^{2+}$, $Cu^{2+}$, and $Pb^{2+}$ is favorable at high temperature thus confirming that adsorption process is endothermic. Such a situation is better explained by thermodynamic adsorption parameters like enthalpy change ($\Delta H°$), entropy change ($\Delta S°$) and Gibb's free energy change ($\Delta G°$) which are easily determined by change in equilibrium constant $K$ with temperature. Value of $K$ is obtained as:

$$K = \frac{C_1}{C_2} \tag{8}$$

where $C_1$ is quantity of metal ion adsorbed per unit mass of erionite and $C_2$ is the aqueous phase concentration of metal ion. From slope and intercept the of Van't Hoff plot thermodynamic parameters like enthalpy change ($\Delta H°$) and entropy change ($\Delta S°$) were determined. In Van't Hoff plot ln$K$ is plotted against $1/T$ using following equation:

$$\ln K = \frac{\Delta S°}{R} - \frac{\Delta H°}{RT} \tag{9}$$

Gibb's free energy change ($\Delta G°$) was calculated by using following equation:

$$\Delta G° = -RT\ln K \tag{10}$$

Thermodynamic parameter for metal ion adsorption on erionite is given in Table. 4. Gibb's free energy ($\Delta G°$) values of $Cd^{2+}$, $Cu^{2+}$, and $Pb^{2+}$ were found to be negative which show spontaneity and feasibility of adsorption for all the three metal ions on erionite. Further the enthalpy change ($\Delta H°$) of $Cd^{2+}$, $Cu^{2+}$, and $Pb^{2+}$ was found to be positive thus confirming adsorption to be endothermic.

## 4. Conclusion

Nanocrystalline erionite was synthesized with an aim to apply it as an adsorbent against aqueous metal ion pollutants. The synthesized erionite was characterized by various sophisticated techniques to understand its surface properties before using it as sorbent against selected metal

Table 2
Isotherm models parameters for metal ions adsorption onto erionite

| Metal ion | Temperature (°C) | Langmuir isotherm model | | | | | Freundlich isotherm model | | | | |
|---|---|---|---|---|---|---|---|---|---|---|---|
| | | $q_{max}$ (mg/g) | $K_L$ (L/mg) | $R^2$ | RMSE | SD | $K_F$ (mg/g) (L/mg)$^{1/n}$ | $1/n$ | $R^2$ | RMSE | SD |
| $Cu^{2+}$ | 30 | 123.17 | 0.04 | 0.94 | 0.08 | 0.16 | 36.15 | 0.26 | 0.98 | 0.04 | 0.04 |
| | 40 | 179.06 | 0.04 | 0.94 | 0.04 | 0.09 | 33.28 | 0.34 | 0.99 | 0.02 | 0.03 |
| | 50 | 265.41 | 0.05 | 0.93 | 0.02 | 0.05 | 39.93 | 0.36 | 0.98 | 0.03 | 0.04 |
| $Cd^{2+}$ | 30 | 134.47 | 0.03 | 0.95 | 0.04 | 0.10 | 26.75 | 0.18 | 0.99 | 0.02 | 0.03 |
| | 40 | 196.9 | 0.04 | 0.96 | 0.04 | 0.11 | 22.21 | 0.16 | 0.99 | 0.03 | 0.03 |
| | 50 | 258.71 | 0. 04 | 0.94 | 0.08 | 0.16 | 35.11 | 0.22 | 0.98 | 0.03 | 0.04 |
| $Pb^{2+}$ | 30 | 141.41 | 0.05 | 0.95 | 0.04 | 0.09 | 42.23 | 0.28 | 0.97 | 0.05 | 0.05 |
| | 40 | 193.61 | 0.04 | 0.97 | 0.03 | 0.07 | 56.52 | 0.35 | 0.99 | 0.02 | 0.03 |
| | 50 | 275.73 | 0. 05 | 0.95 | 0.04 | 0.09 | 61.32 | 0.39 | 0.99 | 0.03 | 0.03 |

Table 3
Comparison of adsorption capacity of erionite for $Cu^{2+}$, $Cd^{2+}$, and $Pb^{2+}$ ions

| Adsorbents | $q_m$ (mg/g) | | | References |
|---|---|---|---|---|
| | $Cu^{2+}$ | $Cd^{2+}$ | $Pb^{2+}$ | |
| Erionite | 265.41 | 258.71 | 275.73 | This work |
| $Fe_3O_4$/LDH-AM | 64.66 | 74.06 | 266.6 | [23] |
| Carboxylated cellulose nanofibrils-filled magnetic chitosan hydrogel beads | | | 171.0 | [24] |
| Magnetic hydrogel beads based on poly(vinyl alcohol)/carboxymethyl starch-g-poly(vinyl imidazole) | 83.60 | 53.20 | 65.00 | [25] |
| Hydrous zirconium oxide-impregnated chitosan beads | | | 222.2 | [26] |
| Chitosan/rectorite nano-hybrid composite microspheres | 20.49 | 16.53 | | [27] |
| Phosphate-embedded calcium alginate beads | | 82.64 | 263.2 | [28] |
| Porous attapulgite/polymer beads | 25.30 | 32.70 | | [29] |
| Oiltea shell | 7.42 | 18.02 | 4.17 | [30] |

Table 4
Thermodynamics parameter of $Cu^{2+}$, $Cd^{2+}$, and $Pb^{2+}$ adsorption on erionite

| Metal ion | Temperature | Equilibrium constant ($K_{eq}$) | Free energy ($\Delta G°$) | Enthalpy ($\Delta H°$) | Entropy ($\Delta S°$) |
|---|---|---|---|---|---|
| Units | °C | Dimensionless | kJ/mol | kJ/mol | kJ/K/mol |
| $Cu^{2+}$ | 30 | $1.885 \times 10^3$ | –22.5891 | | |
| | 40 | $2.572 \times 10^3$ | –24.9365 | 63.0537 | 0.24191 |
| | 50 | $3.894 \times 10^3$ | –29.4109 | | |
| $Cd^{2+}$ | 30 | $1.935 \times 10^3$ | –23.9324 | | |
| | 40 | $2.680 \times 10^3$ | –25.7890 | 68.4259 | 0.26032 |
| | 50 | $3.791 \times 10^3$ | –28.7826 | | |
| $Pb^{2+}$ | 30 | $2.013 \times 10^3$ | –24.0807 | | |
| | 40 | $2.981 \times 10^3$ | –27.5674 | 71.7905 | 0.28561 |
| | 50 | $4.506 \times 10^3$ | –29.7650 | | |

ions (Cd, Cu, and Pb). The sorption of the metal ions onto erionite was found to be increasing with an increase in contact time before the equilibrium achieved. The sorption of the metal ions onto erionite was found to be pH-dependent; it was raised with the rise in pH up to optimum pH then either remain unchanged or decreased with further rise. The maximum sorption of $Cd^{2+}$, $Cu^{2+}$, and $Pb^{2+}$ ions on synthesized erionite was found at pH between 6.0 and 8.0. Experimental data was found to fit well in both Langmuir and Freundlich isotherms, but Freundlich model was best according to $R^2$,

RMSE, and SD values. According to Langmuir, the highest uptakes for $Cd^{2+}$, $Cu^{2+}$, and $Pb^{2+}$ metal ions at 50°C were 258.71, 265.41, and 275.73 mg/g, respectively. Upon comparison of erionite with the previously used adsorbents in the literature, its removal capacity has been found to be quite high. These studies will pave a way for other researchers to prepare new mica minerals to be used as adsorbents.

## References


[1] P. Soderland, S. Lovekar, D.E. Weiner, D.R. Brooks, J.S. Kaufman, Chronic kidney disease associated with environmental toxins and exposures, Adv. Chronic Kidney Dis., 17 (2010) 254–264.

[2] J. Pan, J.A. Plant, N. Voulvoulis, C.J. Oates, C. Ihlenfeld, Cadmium levels in Europe: implications for human health, Environ. Geochem. Health, 32 (2010) 1–12.

[3] L. Liu, H. Chen, P. Cai, W. Liang, Q. Huang, Immobilization and phytotoxicity of Cd in contaminated soil amended with chicken manure compost, J. Hazard. Mater., 163 (2009) 563–567.

[4] H. Hu, R. Shih, S. Rothenberg, B.S. Schwartz, The epidemiology of lead toxicity in adults: measuring dose and consideration of other methodologic issues, Environ. Health Perspect., 115 (2007) 455–462.

[5] E. Obi, D.N. Akunyili, B. Ekpo, O.E. Orisakwe, Heavy metal hazards of Nigerian herbal remedies, Sci. Total Environ., 369 (2006) 35–41.

[6] C. Behera, R. Rautji, T.D. Dogra, An unusual suicide with parenteral copper sulfate poisoning, Med. Sci. Law, 47 (2007) 357–358.

[7] G. Cimino, A. Passerini, G. Toscano, Removal of toxic cations and Cr(VI) from aqueous solution by hazelnut shell, Water Res., 34 (2000) 2955–2962.

[8] A.A. Abia, M. Horsfall, O. Didi, The use of chemically modified and unmodified cassava waste for the removal of Cd, Cu and Zn ions from aqueous solution, Bioresour. Technol., 90 (2003) 345–348.

[9] P.A. Brown, S.A. Gill, S.J. Allen, Metal removal from wastewater using peat, Water Res., 34 (2000) 3907–3916.

[10] M. Danish, R. Hashim, M.N.Mohamad Ibrahim, O. Slaiman, Optimized preparation for large surface area activated carbon from date (*Phoenix dactylifera* L.) stone biomass, Biomass Bioenergy, 61 (2014) 167–178.

[11] V.C. Srivastava, I.D. Mall, I.M. Mishra, Removal of cadmium(II) and zinc(II) metal ions from binary aqueous solution by rice husk ash, Colloids Surf., A, 312 (2008) 172–184.

[12] M. Huang, Z. Li, B. Huang,N. Lou, Q. Zhang, X. Zhai, G. Zeng, Investigating binding characteristics of cadmium and copper to DOM derived from the compost and rice straw using EEM-PARAFAC combind with two-dimensional FTIR correlation analyses, J. Hazard. Mater., 344 (2018) 539–548.

[13] C.G. Rocha, D.A.M. Zaia, R.V. da Silva Alfaya, A.A. da Silva Alfaya, Use of rice straw as biosorbent for removal of Cu(II), Zn(II), Cd(II) and Hg(II) ions in industrial effluents, J. Hazard. Mater., 166 (2009) 383–388.

[14] T.K. Naiya, P. Chowdhury, A.K. Bhattacharya, S.K. Das, Saw dust and neem bark as low-cost natural biosorbent for adsorptive removal of Zn(II) and Cd(II) ions from aqueous solutions, Chem. Eng. J., 148 (2009) 68–79.

[15] X. Xu, X. Cao, L. Zhao, H. Wang, H. Yu, B. Gao, Removal of Cu, Zn, and Cd from aqueous solutions by the dairy manure-derived biochar, Environ. Sci. Pollut. Res., 20 (2013) 358–368.

[16] A.Z.M. Badruddoza, Z.B.Z. Shawon, W.J.D. Tay, K. Hidajat, M.S. Uddin, $Fe_3O_4$/cyclodextrin polymer nanocomposites for selective heavy metals removal from industrial wastewater, Carbohydr. Polym., 91 (2013) 322–332.

[17] D.J.L. Guerra, J. Goco, J. Nascimento, I. Melo, Adsorption of divalent metals on natural and functionalized nontronite hybrid surfaces: an evidence of the chelate effect, J. Saudi Chem. Soc., 20 (2016) S552–S565.

[18] I. Mobasherpour, E. Salahi, M. Pazouki, Removal of nickel(II) from aqueous solutions by using nano-crystalline calcium hydroxyapatite, J. Saudi Chem. Soc., 15 (2011) 105–112.

[19] T. Motsi, N.A. Rowson, M.J.H. Simmons, Adsorption of heavy metals from acid mine drainage by natural zeolite, Int. J. Miner. Process., 92 (2009) 42–48.

[20] A.A. Shyaa, O.A. Hasan, A.M. Abbas, Synthesis and characterization of polyaniline/zeolite nanocomposite for the removal of chromium(VI) from aqueous solution, J. Saudi Chem. Soc., 19 (2015) 101–107.

[21] W.A. Khanday, S.K. Singh, J. Bhaudoriya, S.A. Majid, S.S. Tomar, R. Tomar, Study of sorption of $Pb^{2+}$, $Cd^{2+}$, $Zn^{2+}$, and $Cu^{2+}$ from wastewater on synthetic analogues of clintonite, Colloid J., 74 (2012) 573–581.

[22] P. Gupta, W.A. Khanday, S.A. Majid, V. Kushwa, S.S. Tomar, R. Tomar, Study of sorption of metal oxoanions from waste water on surfactant modified analog of laumontite, J. Environ. Chem. Eng., 1 (2013) 510–515.

[23] J. Sun, Y. Chen, H. Yu, L. Yan, B. Du, Z. Pei, Removal of $Cu^{2+}$, $Cd^{2+}$ and $Pb^{2+}$ from aqueous solutions by magnetic alginate microsphere based on $Fe_3O_4$/MgAl-layered double hydroxide, J. Colloid Interface Sci., 532 (2018) 474–484.

[24] Y. Zhou, S. Fu, L. Zhang, H. Zhan, M.V. Levit, Use of carboxylated cellulose nanofibrils-filled magnetic chitosan hydrogel beads as adsorbents for Pb(II), Carbohydr. Polym., 101 (2014) 75–82.

[25] Z.S. Pour, M. Ghaemy, Removal of dyes and heavy metal ions from water by magnetic hydrogel beads based on poly(vinyl alcohol)/carboxymethyl starch-g-poly (vinyl imidazole), RSC Adv., 5 (2015) 64106–64118.

[26] D.W. Cho, B.H. Jeon, Y. Jeong, I.H. Nam, U.K. Choi, R. Kumar, H. Song, Synthesis of hydrous zirconium oxide-impregnated chitosan beads and their application for removal of fluoride and lead, Appl. Surf. Sci., 372 (2016) 13–19.

[27] L. Zeng, Y. Chen, Q. Zhang, X. Guo, Y. Peng, H. Xiao, X. Chen, J. Luo, Adsorption of Cd(II), Cu(II) and Ni(II) ions by cross-linking chitosan/rectorite nano-hybrid composite microspheres, Carbohydr. Polym., 130 (2015) 333–343.

[28] Y.Y. Wang, W.B. Yao, Q.W. Wang, Z.H. Yang, L.F. Liang, L.Y. Chai, Synthesis of phosphate-embedded calcium alginate beads for Pb(II) and Cd(II) sorption and immobilization in aqueous solutions, Trans. Nonferrous Met. Soc. China, 26 (2016) 2230–2237.

[29] Y. Feng, Y. Wang, Y. Wang, S. Liu, J. Jiang, C. Cao, J. Yao, Simple fabrication of easy handling millimeter-sized porous attapulgite/polymer beads for heavy metal removal, J. Colloid Interface Sci., 502 (2017) 52–58.

[30] J. Liu, C. Hu, Q. Huang, Adsorption of $Cu^{2+}$, $Pb^{2+}$, and $Cd^{2+}$ onto oiltea shell from water, Bioresour. Technol., 271 (2019) 487–491.

[31] W.A. Khanday, S.A. Majid, S.C. Shekar, R. Tomar, Synthesis and characterization of various zeolites and study of dynamic adsorption of dimethyl methyl phosphate over them, Mater. Res. Bull., 48 (2013) 4679–4686.

[32] W.A. Khanday, Dynamic cum batch adsorption of a vesicant CWA (2-chloroethyl ethyl sulfide) over synthetic erionite, Microporous Mesoporous Mater., 244 (2017) 15–20.

[33] I. Langmuir, The adsorption of gases on plane surfaces of glass, mica and platinum, J. Am. Chem. Soc., 40 (1918) 1361–1403.

[34] H. Freundlich, Uber die adsorption in losungen, Z. Phys. Chem., 57 (1906) 385–470.

[35] V.O. Njoku, M.A. Islam, M. Asif, B.H. Hameed, Preparation of mesoporous activated carbon from coconut frond for the adsorption of carbofuran insecticide, J. Anal. Appl. Pyrolysis, 110 (2014) 172–180.

[36] L. Shen, J. Wang, Z. Li, L. Fan, R. Chen, X. Wu, J. Li, W. Zeng, A high-efficiency $Fe_2O_3$@microalgae composite for heavy metal removal from aqueous solution, J. Water Process Eng., 33 (2020) 101026, doi: 10.1016/j.jwpe.2019.101026.

[37] Q. Chen, Z. Tang, H. Li, M. Wu, Q. Zhao, B. Pan, An electron-scale comparative study on the adsorption of six divalent heavy metal cations on $MnFe_2O_4$@CAC hybrid: experimental and DFT investigations, Chem. Eng. J., 381 (2020) 122656, doi: 10.1016/j.cej.2019.122656.